Chapter 1

Introduction

Employing of the contemporary technologies has become a leading part of the present era and has been motivating the preceding research on the finding of new multifunctional materials with novel properties. The discovery of such new materials with versatile applications has immense significance in today's life, influencing our relationships in many aspects i.e., health care, data and energy saving, communications, and many more. In this regard, magnetism is particularly one of the most extensive interests in contemporary technologies. In everyday life, magnetism is employed in various aspects of life such as the read-heads, magnetic memory storage, transformers, and television. The advanced technology evolved from video tape and cassettes to pen drives, computer hard disks, and also debit/credit cards, magnetism surely plays a significant role. However, the unravelling of the new multifunctional materials which countered various external stimuli provides a new vision in material research and enhances the advanced future technology of spintronic devices. Therefore, recently, the invention of such systems has gotten particular attention because their novel properties can be applied to build innovative technological applications such as memory devices, spin switching, spin-filters, etc.

1.1 A brief Introduction to magnetism:

Magnetic materials have ion that contains magnetic moment and are expressed as the sum of both spin and orbital motion of the electron as well as their interaction with each other. However, the magnetic moment generated by the nucleons is negligibly lesser as compared to the magnetic moment due to the electron. Thus, the magnetism of material is entirely related to the electronic configuration of the particular ions. As a result, if all the electrons in any element are paired with each other than the magnetic spins will cancel one another giving rise to zero magnetic moments. In contrast, when at least one electron remains unpaired in the ion leading to the net magnetic moment. These magnetic materials interact differently with an external magnetic field. On this basis, magnetic materials can be

commonly classified into the following types, i.e., diamagnetic (DM), paramagnetic (PM), ferromagnetic (FM), antiferromagnetic (AFM), and ferrimagnetic (FIM).

1.1.1 Diamagnetic materials:

DM property of a material is described by the feeble rise in the magnetization in the opposite direction of the applied magnetic field hence giving rise to the negative susceptibility. Diamagnetism can be understood by Lenz's law according to the classical viewpoint viz., the change in the applied magnetic field produces an electromotive force opposing the applied magnetic field by the orbital motion of the electron. Whereas, according to quantum mechanics, all materials have intrinsic diamagnetism. All the electrons in the DM materials are fully paired thus leading to zero net magnetic moments.

1.1.2 Paramagnetic materials:

PM materials exhibit small positive susceptibility in contrast to the DM materials. In these materials, the spins align parallel to the applied magnetic field giving rise to a net magnetic moment because of the unpaired electrons. The spins are randomly aligned without any applied magnetic field since their interaction with each other is merely present. However, under the application of the magnetic field, some spins are aligned although the alignment of the spins or the induced magnetization depends upon two parameters: the ability of the magnetic field under application and temperature. The increase in the strength of the magnetic field which is applied tends to increment the degree of alignment while the increment in the temperature tends to increase the randomness of the spins by increasing the thermal fluctuations. Theoretically, it is defined by the partition function.

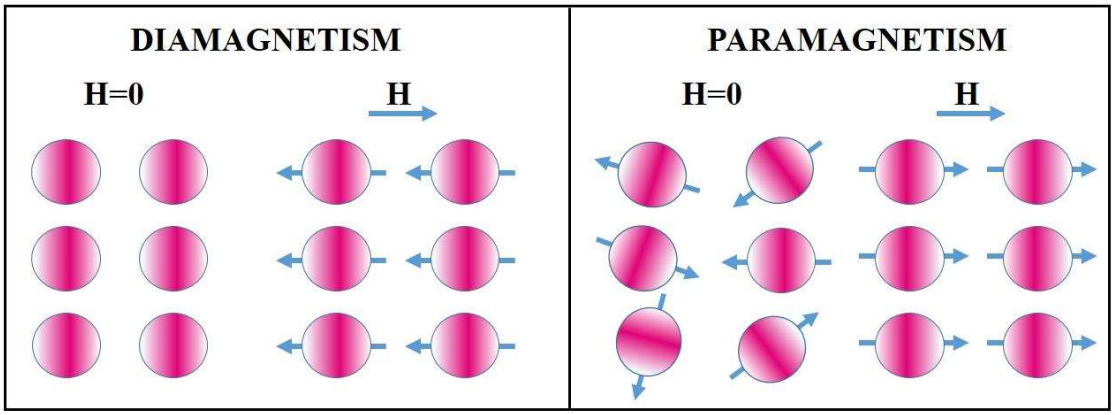

Fig. 1.1: The schematic spin alignments for diamagnetism and paramagnetism microscopic structures in the presence and absence of magnetic field H.

The partition function of the system having N free spins can be described as follows according to the canonical ensemble

$$Z = \Sigma e^{-\beta \mu_i H} \tag{1.1}$$

Where μ_i known as the magnetic moment of i ions and β known as the Boltzmann's constant [1], [2].

Whereas, the magnetic moment aligned along j direction can be expressed as

$$\mu_j = g_{jk} S_k \mu_B \tag{1.2}$$

Where, g_{jk} is known as the Lange g's factor, S_k is known as the total angular momentum, k is known as the spatial direction and μ_B is known as the Bohr magneton [3]. Fig. 1.1 demonstrates the spin arrangement for the DM and PM materials in the presence and absence of a magnetic field.

1.1.3 Ferromagnetic materials:

FM materials exhibit large and positive magnetic susceptibility since they are strongly influenced by the application of the magnetic field. The spins are aligned parallelly to each

other in these materials. Moreover, FM materials sustain their magnetization after removing the applied magnetic field due to their inherent property. FM materials lead to the generation of magnetic domains due to the minimization of the free energy of the system. These magnetic domains aligned randomly in the absence of any magnetic field in FM materials. In contrast, under the application of the magnetic field, all the magnetic moments orient parallelly in the same direction, and even after removing the magnetic field some of the domains still prevail in the same direction and give rise to the remanent magnetization along with the hysteresis loop.

1.1.4 Antiferromagnetic materials:

The AFM materials have antiparallelly aligned sublattice to each other with equal magnetic moments. As a consequence, AFM systems have zero net moments as they mutually cancel each other's magnetic moments.

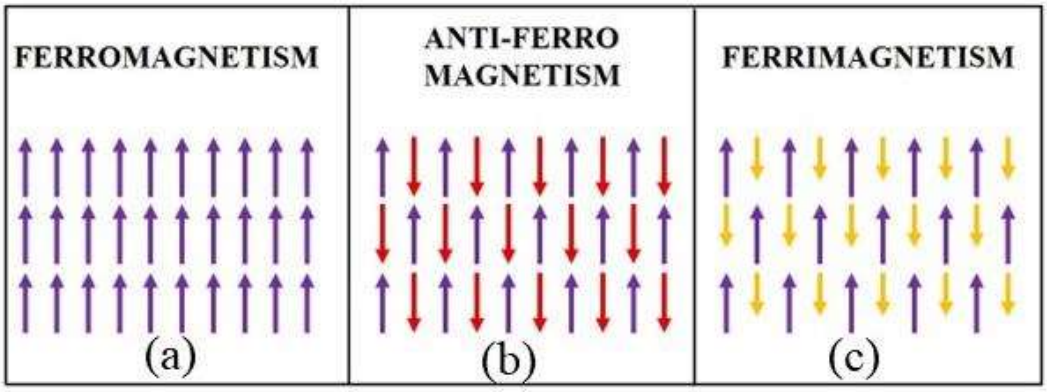

Fig. 1.2: The spontaneous spin alignments for (a) ferromagnet (b) an antiferromagnet (c) a ferrimagnet below a critical temperature called magnetic ordering temperature.

.

1.1.5 Ferrimagnetic materials:

FIM materials contain both ferromagnetism and antiferromagnetism properties in the same system. In ferrimagnetism, sublattices are aligned antiparallel to neighboring sublattices as AFM materials yet the sublattices have a difference in the magnitude of the magnetic moment. Thus, it exhibits a net non-zero magnetic moment. Fig. 1.2 describes the spin arrangement of FM, AFM, and FIM materials below the critical temperature.

1.2 Rules define the different types of magnetic ordering:

1.2.1 Curie – Weiss Law:

The magnetization is stated as below according to the Langevin PM theory:

$$M = NmL\left(\frac{\mu_0 mH}{k_B T}\right) = Nm\left[coth\left(\frac{\mu_0 mH}{k_B T}\right) - \frac{k_B T}{\mu_0 mH}\right] \quad (1.3)$$

Under the large magnetic field ($\mu_0 mH \gg k_B T$), M = Nm; at high temperature ($\mu_0 mH \ll k_B T$), $M = \mu_0 Hm^2 H/3K_B T$. Langevin function is modified by the Brillouin function after considering the spatial quantization, and susceptibility is converted:

$$\chi_{PM} = \frac{M}{H} = \mu_0 \frac{Ng^2 J(J+1)\mu_B}{3k_B T} = \frac{C}{T} \quad (1.4)$$

This is known as Curie-Weiss (CW) law for paramagnetism, here N represents the number of atoms per unit volume K_B is known as the Boltzmann constant. CW law for the FM is defined as:

$$\chi_{FM} = \frac{C}{T - T_C} \quad (1.5)$$

Similarly, the susceptibility for AFM and FIM is defined by Neel and known as Curie-Neel law:

$$\chi_{AFM} = \frac{C}{T + T_N} \quad (1.6)$$

$$\chi_{FIM} = \frac{T+C/\chi_0}{C} - \frac{b}{T-\theta} \tag{1.7}$$

We have shown the behavior of the susceptibility and inverse magnetic susceptibility with temperature in Fig. 1.3 for different materials.

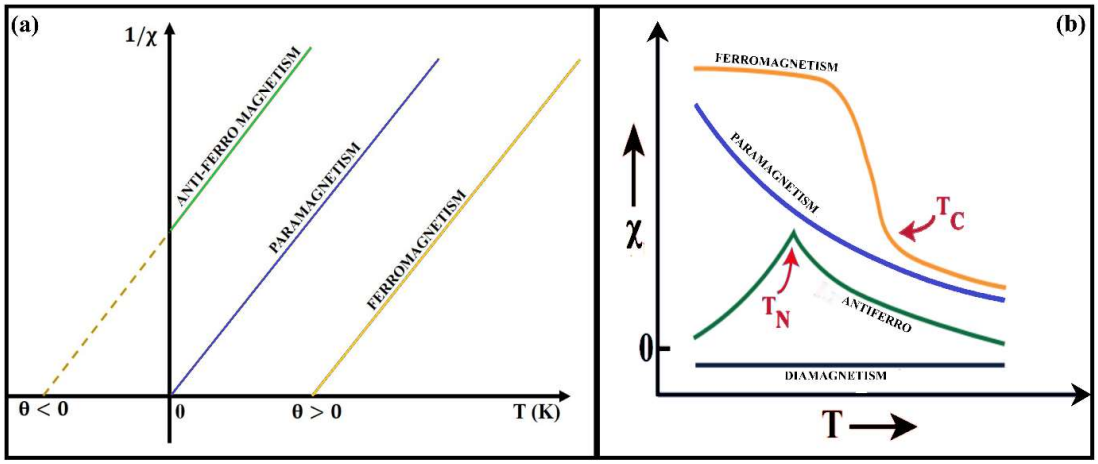

Fig. 1.3: (a) and (b) show the thermal variation of inverse magnetic susceptibility and magnetic susceptibility for PM, FM, and AFM material, respectively.

1.2.2 Landau's theory of ferromagnetism (mean field theory):

Free energy is expressed as:

$$F(M) = F_0 + a(T)M^2 + bM^4 \tag{1.8}$$

Where F_0 and b are the constants (b>0) and $a(T)$ is the temperature-dependent parameter. The proper phase transition occurred when $a(T)$ becomes: $a(T) = a_0(T - T_c)$, where a_0 is known as the proper constant.

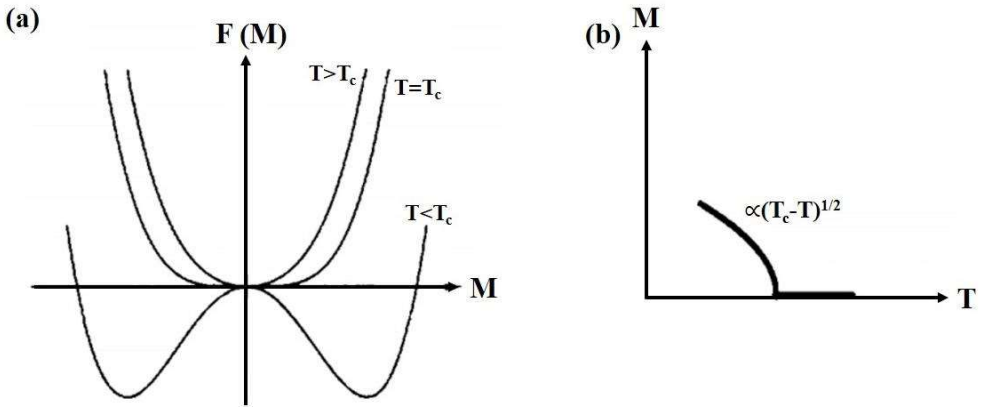

Fig. 1.4:(a) Free energy vs. magnetization curve. (b) Magnetization vs. temperature graph.

For the minimization of the free energy:

$$\frac{\partial F}{\partial M} = 0 \tag{1.9}$$

$$2M[a_0(T - T_c) + 2bM^2]$$

$$M = 0 \; or \; M = \pm\left[\frac{a_0(T - T_c)}{2b}\right]^{1/2}$$

The first term is applicable for the above and below T_c while the second term is considered only below T_c. It provides an unstable equilibrium $\left(\frac{\partial^2 F}{\partial^2 M}\right)$ for $T < T_c$. Thus, below T_c, the magnetization is proportional to $(T_c - T)^{1/2}$ as shown in Fig. 1.4 along with the variation of free energy with magnetization [4] .

1.2.3 Heisenberg Model:

The Heisenberg model explained the configuration of different magnetic systems and the total energies of the system can be expressed as:

$$H = -\Sigma_{<ij>} J_{ij} S_i S_j \tag{1.10}$$

Where J is known as the exchange constant, S_i and S_j are known as Pauli matrices. The spins are considered quantum mechanically according to this model. The Heisenberg model is applicable for phase transition as well as the critical points of magnetic systems.

1.2.4 Ising Model:

The Ising model considered the movement of the spin only in an upward or downward direction. Thus, only the z component of the spins is included in this model and can be expressed as:

$$H = -\Sigma_{<ij>} J_{ij} S_i^z S_j^z \tag{1.11}$$

Where, S^z is known as the operator for only the z component of the spins. The phase transition does not take place when the Ising spins are aligned as in a one-dimensional (1D) lattice. In addition, the Hamiltonian for N+1 spins are written as:

$$H = -2J\Sigma_{i=1}^{N} J_{ij} S_i^z S_{i+1}^z \tag{1.12}$$

1.2.5 Landau's theory of phase transition:

Landau's theory describes the nature of FM materials near the magnetic phase transition temperature T_C. The magnetization below T_C, at T_C, and above T_C varies as:

$$\chi \propto (T - T_C)^{-\gamma}, \text{ T>T}_C \tag{1.13}$$

$$M \propto (T_C - T)^{\beta}, \text{ T<T}_C \tag{1.14}$$

$$M \propto H^{1/\delta}, \text{ T = T}_C \tag{1.15}$$

Where, γ, β and δ are known as the critical exponents. The value of these critical exponents suggests the nature of the phase transition. The following list describes the different values of critical exponent according to a different model:

Exponent	Mean field Model	Ising Model	Heisenberg Model
D	Any	1	3
D	Any	2	3
B	1/2	1/8	0.367
Γ	1	7/4	1.388
Δ	3	1.5	4.78

1.3 Spin Frustration:

In condensed matter physics, frustration has arisen in any lattice when it is not able to satisfy all the interactions and does not reach the single ground state. According to the third law of thermodynamics, at thermodynamic equilibrium, the entropy of a system attains the fixed value as the temperature is at absolute zero. However, the above condition leads to multiple ground states with similar low energy instead of a unique single ground state. In this case, these systems can alter between different states. These systems are known as spin frustrated systems. Intriguingly, such frustration between the spins is the magnification of the different magnetic phenomena observed in the frustrated system in magnetism. In magnetism, P. W. Anderson initially used the frustration word and later on adapted it to describe several interesting phenomena [5]. Spin frustration is observed in several systems such as liquid crystals, molecular crystals, magnetic thin films, and even in superconducting Josephson junction arrays. In condensed matter physics, disorder-driven spin frustration is extensively studied spin frustration.

1.3.1 Disorder-driven Spin Frustration:

Disorder-driven spin frustration is occurred due to the randomness or disorderness in any system. This results in altering the magnetic nature of the system which further leads to

interesting phenomena such as the formation of re-entrant cluster glass/re-entrant spin glass (RCG/RSG) state at low temperature, colossal exchange bias (EB), metamagnetic transition, Griffith-like phase (GP), giant magneto-dielectric coupling (MDC), increment in the magnetocaloric and magnetoresistance effects, etc [6]–[13]. The disorder in the system may occur in various forms viz chemical disorder, site disorder or caused by the structural distortion, etc. The long-range ordering (LRO) is presented in the system when there is a high degree of structural order (except for the lattices which have geometrical frustration). Whereas, the random exchange interaction is created by the disorder further leading to glassy behaviour at low temperatures in which spins are frozen in a non-collinear and random manner. These interactions have randomness in the strength in such a manner that they will lead to competing FM and AFM configurations. That eventually has a beautiful well-known effect on the magnetic behaviour by inducing a new exotic state instead of a single magnetic ground state. Perovskite and double perovskite (DP) materials are famously known to have disorder-driven spin frustration due to the unavoidable quenched disorder which creeps into the system during sample preparation or due to the random substitution of different atoms.

1.3.1.1 Double Perovskite Materials:

The DP materials have immense attention in condensed matter physics for both theoretical and experimental aspects for exploring disorder-induced exotic properties. The name perovskite comes from the mineral, first observed by Gustav Rose in 1839 and named after L. A. Perovski, the famous Russian mineralogist. The usual formula for perovskite is ABO_3 cubic structure, where A is the cation of a larger ionic radius (in general alkaline or rare earth element) as compared to B which is also a cation with a smaller ionic radius generally 3d, 4d, or 5d transition elements. Fig. 1.5 illustrates the structure in which A present at the corners of the cube i.e., (0, 0, 0), while the center of the cube is occupied by B i.e., at the

body-centered position (0.5, 0.5, 0.5) and oxygen atoms are positioned at face centered i.e., (0.5, 0.5, 0.5). B cations are forming an octahedral coordinated by neighboring oxygen atoms while A cations sustain cuboctahedral coordination with 12-fold. As the name suggests, the ordered DP is formed with two perovskites viz $ABO_3.AB'O_3$ ($A_2BB'O_6$) in which both the unit cell of single perovskite repeat itself in an alternative manner appeared as a checkerboard type pattern as demonstrated in Fig. 1.5 [14].

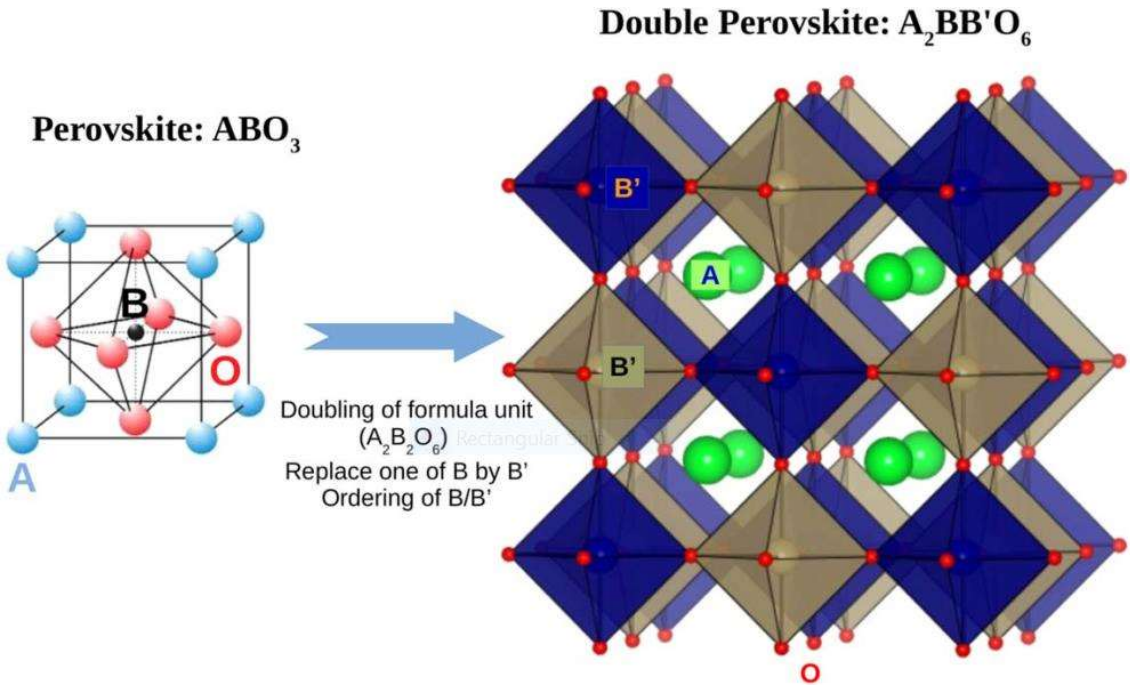

Fig. 1.5: Pictorial diagram of a double perovskite unit cell, initiated with a perovskite unit cell.

The B-site cation ordering and consecutive oxidation state is the main reason for the peculiar and novel ground state of the DPs family. In general, the DPs with B-site having Co/Mn/Ni transition metals have laid in the category of the ordered DPs showed FM ground state can be described by the 180° superexchange interaction between B^{2+}/B^{4+} cations through nearest oxygen cation according to Goodenough-Kanamori rules [15], [16].

Although, a perfectly ordered DPs structure is a fascinating platform to theoretically examine its properties, however, it is quite difficult to synthesize a fully ordered structure. During the sample preparation, the disorder comes into the system in form of ASD by exchanging the B/B' cations inevitably. B-site ions ordering decides the structure of DPs, in general, DPs are crystalline in the following two types of structures: (1) the ordered structure formed in the monoclinic phase P_{21}/n spacegroup (2) the B-site disordered structure formed in orthorhombic phase with Pnma spacegroup [17], [18]. Thus, the ordered DP structure is formed by B/B' ions when B-site ions have relatively large ionic radius differences at the same time difference in charge state. On the other hand, B-site disorder is exhibited when the same charges at B-site ions. Furthermore, B^{3+}/B'^{3+} ions create disorder resulting in competition for AFM interactions in the system. Whereas, even though the various study and meticulous observations on similar DPs, a complete understanding of their electronic structure are still not fully understood.

1.3.2 Spin Chain:

The understanding of the quantum phase transitions occurring at low temperatures becomes clearer by studying the low-dimensional and frustrated spin systems [19], [20]. In the early days of quantum mechanics, the understanding of Quantum spin chains was restricted to different models. Later in the 1960s, the experimental realization of the spin chain system was first observed in transition metal salts [21]–[23] which was then explored in other novel materials also [24]–[28]. Despite their simplicity, these spin chain systems display complex nature and properties, such as magnetism [29], [30], short and long-range order [31] entanglement [32], and quantum phase transitions [19], [33]–[35] and topological order [36], [37]. Continuing the research in the field of quantum spin chain systems, Haldane investigated the topological origin of the exotic nature of integer and half-integer spin chains for which he was awarded the Noble prize in 2016 [38], [39].

Spin chain systems have a 1D array of spins. If the individual spins are constrained to move only in parallel or antiparallel of a particular direction then it is known as Ising spin, if they are free to move on a fixed plane then they are called XY spins, and if they can move in any direction then they are known as Heisenberg spins. The magnetic moment can behave according to Ising spins (D = 1), XY spins (D = 2), and Heisenberg spins and can also be oriented in a different way other than the three ways discussed. All arrangements of magnetic spins arise due to the single ion anisotropy as a result of the crystal field. Furthermore, the magnetic LRO is not allowed in the 1D AFM spin chains at zero temperature due to the large quantum fluctuations, thus leading to the gapless excitation spectrum and power-law decay of spin-spin interactions [40]. Nonetheless, at finite temperature, the inherent inter-chain interactions in the real materials, result in the formation of magnetic LRO [41], [42]. On the contrary, the system also exhibits different fascinating states instead of developing the conventional LRO [20], [43]–[45]. In addition to the quantum fluctuations, the competition between the interactions is observed in a set of compounds, enhancing magnetic frustration in spin chain systems which display a multitude of interesting magnetic ground states [46]–[48]. To realize different exchange coupling and various fascinating phases of matter in 1D spin chain systems, the transition-metal oxides introduce multiple possibilities. There exist different types of spin chain families in condensed matter physics, for example, the $CuGeO_3$ compound is a spin peierls compound. It has a uniform linear spin chain with the opening of a spin gap a structural phase transition and below critical temperature continues lattice dimerization [47]. On the other hand, $(VO)_2P_2O_7$ is an alternating spin chain compound that has two different spin gaps where the first gap is about twice the smaller as the second one [49]. Another family of compounds i.e., A_2CuO_3(A = Ca, Sr) is a spin ½ chain compound which shows covalent insulation other than the spin-charge separation which is an important property for using

them in quantum device applications [50]. Moreover, the $AM_2X_2O_8$ family of compounds is recently explored as a quasi-1D spin chain system that forms a chain by corner edge sharing MO_6 octahedra [51]–[53].

1.3.2.1 Quasi 1D screw-chain compound:

In this section, we will introduce the quasi-1D screw chain compound with the general formula $AM_2X_2O_8$ (A = Ba, Sr, Pb; M = Cu, Co, Ni, Mn; X = V, As) in detail. M is, in general, a magnetic ion that forms an octahedra MO_6 and X in general non-magnetic ion which makes a tetrahedra XO_4. The structure forms a screw chain by edge-sharing of each MO_6 octahedron with two neighboring octahedra as shown in Fig. 1.6. The non-magnetic XO_4 tetrahedra and A^{2+} ions separated the screw chain from each other from its neighboring chains, thus leading to the effective one-dimensional magnetic system. Thus, the interchain magnetic interactions become much stronger than interchain interactions. Fig. 1.6(a) and (b) show the screw chains of two different types: (1) the one screw chain along the 4_1-axis is formed by MO_6 octahedra which rotate anti-clockwise with increasing z. In this, the 4_1 axes are situated at $(x = 1/4, y = 0)$ transforms the M_1 atom which is situated at $(z = 1/8)$ into the $M_2(z = 3/8)$, after that into $M_3(z = 5/8)$, and lastly into the $M_4(z = 7/8)$,(2) In this, the 4_1-axis is parallel to the c-axis and situated at $(x = 1/4, y = 1/2)$ transforms the M_5 atom situated at $(z = 1/8)$ into the $M_6(z = 3/8)$, after that into $M_7(z = 5/8)$, and lastly into the M_8 $(z = 7/8)$, and leads to form a screw chain rotating clockwise with increasing z. Most compounds in this series are crystallized in a tetragonal phase with a centrosymmetric space group and their unit cell is body-cantered.

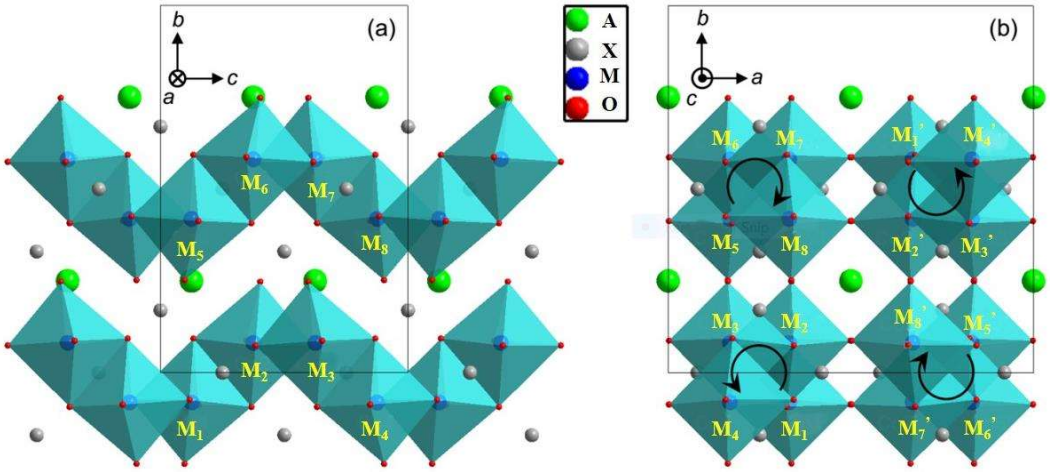

Fig. 1.6: Crystallographic structure of $AM_2X_2O_8$ (a) Projection in the (*b, c*) plane. For better visualization, we have shown only two chains, (b) Projection in the (*a, b*) plane, here, a unit cell composed of four chains is shown. The clockwise and anticlockwise arrows indicate the rotation axis of the screw chains while increasing the *z*.

The real ground state for integer and half-integer spin systems is totally different suggested by Haldane in his pioneer discovery as discussed above [38]. 1D Heisenberg AFM with a half-integer spins system exhibits LRO in the form of power law spin correlations by introducing the slightest disturbance. On the contrary, the ground state is a stable singlet for the integer spin system. Short range ordering (SRO) is exhibited by interachain spin correlation decaying exponentially and leads to a finite energy gap excitation spectrum. While the small magnetic anisotropy and some remaining 3D interaction could not be able to provide magnetism in the system. Thus, the peculiar behavior of the integer spin system has been widely explored theoretically and experimentally. And particularly destroying the singlet ground state after introducing perturbation to establish LRO is recently been extensively studied.

1.4 Fundamental Aspects and Physical Phenomena related to research:

1.4.1 Exchange Interactions:

Magnetic moment arising due to the direct dipole-dipole interaction between electrons is quite small as it cannot be the cause for the standard magnitude of spin-dependent interaction [54]. Therefore, exchange interaction is the fundamental reason for the magnetic properties of a solid when two individual spins are considered. Exchange interactions are the key ingredient for the long-range magnetic ordering of solids. Exchange interaction is associated with the electrostatic interactions between the charges as the same sign cost energy when put close to each other and save energy when placed apart. According to the Pauli exclusion principle, electrons with the same spin at the same point in space have a lesser possibility as compared to the electrons with an opposite spin at the same point in space which is the root of the potential exchange phenomena [55]. Thus, the mean separation r between antiparallel spins is lesser as compared to parallel spins leads to a higher magnitude of Coulomb potential energy ($e^2/4\pi\varepsilon_0 r$) for antiparallel spins. The kinetic energy arises between electrons positioned at two completely different sites. Out of these electrons, one can occupy the site that is filled by another in such a manner that its spin alignment becomes identical with the spin of the unfilled level. This quantum hopping or hybridization of states increases the localized radius resulting in lower kinetic energy. In transition metal compounds the kinetic exchange energy is greater than the potential exchange energy. For any solid, exchange energy is written as:

$$H = -\sum_i \sum_{i \neq j} J_{ij} S_i S_j \tag{1.16}$$

J_{ij} is positive constant for the FM configuration and negative for the AFM configuration. The exchange interaction is related to direct and indirect exchange. Direct exchange interaction arises when the orbital shell of the neighboring magnetic ions overlaps and they

interact via an exchange interaction without the need for any intermediator. In contrast, indirect exchange interaction occurs via a non-magnetic ion between two magnetic ions [56]. In most cases, the indirect exchange has occurred and the most common indirect exchange interaction among all is the superexchange interaction.

1.4.1.1 Superexchange Interaction:

H. Kramers was the first to discuss superexchange interaction in 1934 and later on P. Anderson , J.B.Goodenough, and J. Kanamori shed light on it in 1950-the 1960s [15], [57]–[59] Superexchange interaction is mediated by the non-magnetic ion which is situated in between the magnetic ions with the same valence state. It arises from the electron coming from the same donor atom. This interaction occurred via the 2p level of O^{2-} in the magnetic oxides and due to the favorable kinetic energy of delocalized two bonding electrons of the transition metal ions mediating via O^{2-} ion [60]. Let us consider the Mn^{3+}-O^{2-}-Mn^{3+} bond as demonstrated in Fig. 1.7. The Mn^{3+} has only one unpaired electron in the d orbital whereas the O^{2-} has a filled orbital with two electrons in its outermost shell. Cases 1, 2 and 3 represent the AFM interaction of the ground and excited state configuration (Fig. 1.7) with the accordance of Pauli Exclusion Principle. On the other hand, for the FM interaction, the Pauli Exclusion Principle is not allowed for the excited state as illustrated in cases 3, 4, and 5 (Fig. 1.7). Thus, the superexchange interaction is generally described as AFM interaction. Although the interaction can become FM in some conditions when the transition metal orbitals are coupled at 90° via O^{2-} ion connection or when the bond angle between MOM have enough bending, then the empty orbital and the half-filled orbitals of the metal ions are bridged via oxygen. The plausible superexchange interaction of the ground state configuration is called as Goodenough Kanamori rule as introduced by J. B. Goodenough and J. Kanamori [15].

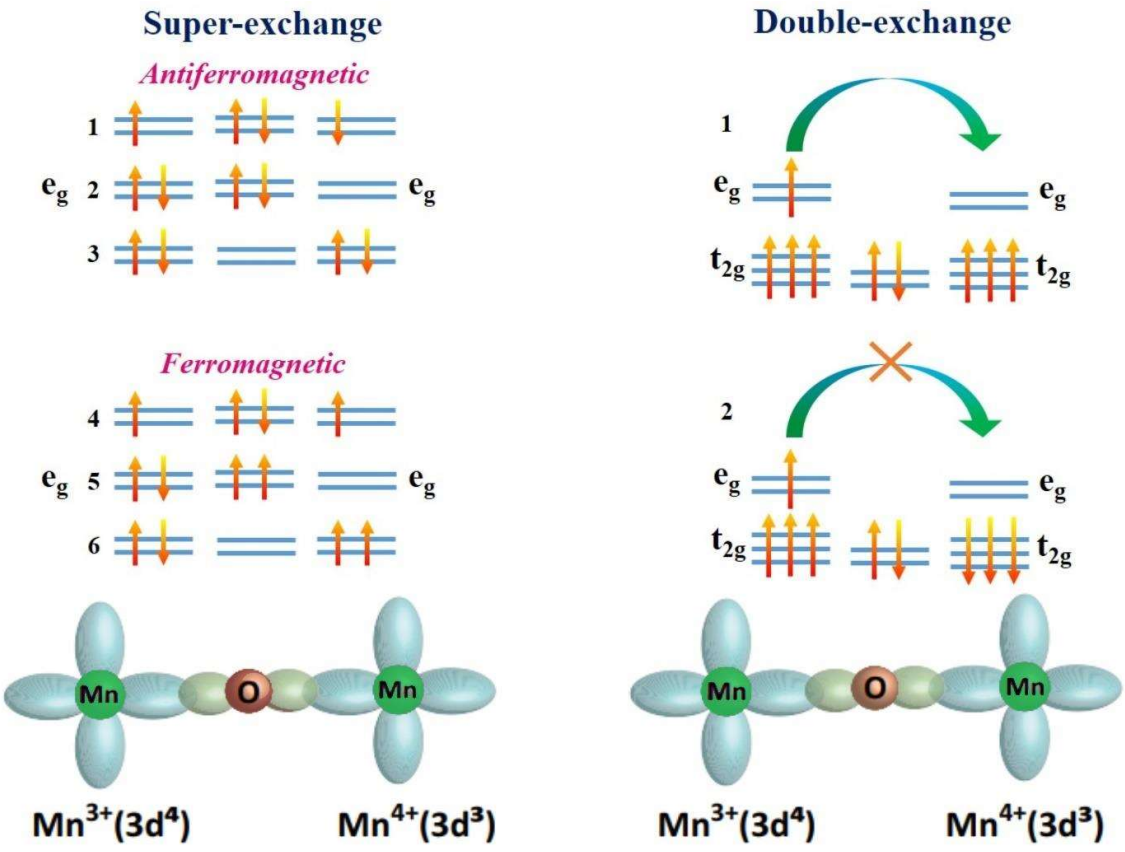

Fig. 1.7: Magnetic indirect exchange interaction. For better clarity Mn^{3+}/Mn^{4+} example was considered.

1.4.1.2 Double Exchange Interaction:

The double exchange interaction was first given by C. Zener and later developed by Anderson [61], [62]. It occurs when the magnetic ion can have a mixed oxidation state i.e., it can reside in more than one valence state and leads to the FM interaction. The ferromagnetism can be interpreted by the hoping of a carrier between nearby unfilled d orbital. The width of the band is proportional to the hopping rate, thus inducing the FM by decreasing the carrier energy since the width is increased. Here, the electron is exchanged between two metals through non-metal i.e., O^{2-} as compared to the superexchange interaction in which actually the electron does not move between the metals. This can be simply demonstrated by considering the system $La_{1-x}Sr_xMnO_3(0 \leq x \leq 1)$, where Mn resides

in Mn^{3+} and Mn^{4+} oxidation states. The double exchange interaction occurs between Mn^{3+}-O^{2-}-Mn^{4+} through the non-metal O^{2-} ions supporting the FM configuration as shown in Fig. 1.7. Since the hopping between the electrons takes place without spin-flip thus if there is a vacancy of the same spin available at the neighboring Mn site then hoping can occur of the e_g electron of Mn^{3+}. Therefore, this scenario is possible when the neighboring site has occupied by Mn^{4+} ion with an empty e_g orbital. The 3 t_{2g} electrons favor the orientation of e_g electrons in the same direction as themselves, according to Hund's rule 1 (case 1, Fig. 1.7). Thus, the FM arrangement is essential for the successful hop between these metals as AFM is not energetically favourable (case 2, Fig. 1.7).

1.4.2. Spin-glass Phase:

Spin glass (SG) is the new field of interest in magnetism where the spins behave differently from the conventional LRO instead of at low temperatures it behaves collectively [63]. The term 'glass' is directly related to normal glass because the alignment of the spins looks randomly but does not change with time in these magnetic phases. Thus, the origin of the name SG is due to the analogous nature of frozen random alignment of spins with frozen particles in a normal glass. The occurrence of the SG phase has mainly these three reasons: competing interactions, randomness, and frustration. The disoderness of glassy behavior occurs due to the following reasons such as site disorder which arises due to the randomization or disorderness of the distance among the magnetic moments, or due to randomization of the nearest neighbor interaction called bond randomness [64]. Moreover, in the system, the randomness in the strength of these interactions along with the mixed FM and AFM interactions causes frustration. Thus, the appearance of magnetic frustration causes by the competition between FM and AFM interactions results in the degenerate multiple magnetic ground state. The time scale evolution of the domain is at the microscopic level in pure FM and AFM systems while due to the glassy behavior, pinning

of the domain wall occurs that further leading to the metastable state. These metastable states involve the domain wall transfer from one state to another through thermal-activated hopping phenomena. In the experimental time scale, the equilibrium state is not achieved by the system during this procedure which is demonstrated by the memory effects, non-exponential decay, aging effects, slow spin-relaxations thermomagnetic irreversibility, etc. Thus, the disorder is the essential ingredient for inducing the glassy phase. In contrast, when spin frustration or disorder is locally present in the area of the cluster known as a cluster glass (CG) phase [65]. The CG phase occurs induce in a system when one of the competing interactions between FM and AFM is stronger compared to the other. Actually, the cluster of spins is a larger entity than atomic spins thus seen as the huge spin moment. Whereas, the RCG phase arises in the system when there is a higher temperature LRO state reaches into the CG phase at low temperature. The complex distinction between these states can be made by the non-linear susceptibility and relaxation experiments [66]. The initial analysis of the nature of glassy behavior is obtained by the various model on the frequency-dependent ac susceptibility measurement as follows:

- **Vogel-Fulcher Model:** In this model, the analysis of the peak temperature of different frequencies gives a basic understanding of glassy behavior [67]. The viscosity of supercooled liquids is discussed by this empirical law as:

$$\tau = \tau_0 \exp\left(-\frac{E_A}{K_B(T_f - T_0)}\right) \qquad 1.17$$

Here, τ_0, E_A and T_0 is the parameters obtained by fitting. T_0 is known as the ideal glass temperature for actual glasses. This model gives more feasible physical parameters as compared to the simple activation fit. The accurate physical meaning of the T_f parameters need more attention.

- **Dynamic-Scaling Model:** In this model standard theory of dynamic scaling is employed near a phase transition temperature [68]. The outcome of the dynamic scaling relates between the critical relaxation time τ and the standard correlation length ζ i.e., $\zeta \sim \tau^2$. ζ diverges with temperature as $\zeta \sim [T_G/(T_f - T_G)]^{\nu}$, thus power law divergence is as follows:

$$\tau = \tau_0 \left(\frac{T_f - T_G}{T_G}\right)^{-z\nu} \quad (1.18)$$

Here, f is the excitation frequency corresponding to the characteristic spin-flip time ($f_0 = \frac{1}{\tau_0}$); T_G is the equivalent spin-glass freezing temperature in the limit of $f \rightarrow 0\ Hz$ and $H_{DC} \rightarrow 0\ Oe$, f_0 is related to the characteristic spin flipping time (τ_0) as $f_0 = \frac{1}{\tau_0}$; zv is the dynamical critical exponent which should be between 4 to 12 for glassy transition.

Another evidence for the slow spin relaxation in the SG or CG phase can be made by the time-dependent measurement of thermo-remanent magnetization (TRM) m(t) in the region of the SG/CG i.e., below the freezing transition temperature T_f and can be fitted by the following model.

- **KWW Model:** Initially the KWW (Kohlrausch Williams Watt) model was come to light in 1854 by R. Kohlrausch in 1854 to discuss the charge of the capacitor (Leyden jar) [69]. Later on, the Fourier transform of the stretched exponential is introduced by Williams and D. C. Watts in 1970 to discuss the dielectric spectra of polymers [70]. The stretched exponential relaxation has been found empirically in various amorphous materials, such as in, for instance, many polymers, glasses, and glass-forming liquids near the glass transition temperature. Nowadays, the KWW

function is extensively employed to discuss a relaxation of various nature, viscosity, friction, gas kinetics, heat transfer, etc. The TRM measurement was performed during the field cooled protocol. The sample is cooled under the application of the magnetic field till the desired temperature and the time-dependent magnetization data are measured after removing the magnetic field completely. The normalized magnetization m(t)=$\frac{M_t}{M_{t=0}}$ has been plotted as a function of time. The time evolution of the TRM can be analyzed using the KWW stretched exponential equation as follows [71], [72]:

$$m(t) = m_0 - m_g exp\left\{-\left(\frac{t}{\tau}\right)^{\beta}\right\} \quad (1.19)$$

Here, m_0 is the initial remanent magnetization, m_g is the magnetization of glassy component, τ is known as the characteristic relaxation time constant and β is the shape parameter or stretching exponent. β value varies between 0 to 1 for disordered systems of different classes.

1.4.3. Griffith Phase:

GP is been an interesting topic of magnetism for the last decade. Griffith introduced a Griffith temperature (T_G) and below this characteristic temperature, the system has the finite size of FM clusters associated with the spin up to the long-range transition temperature T_C. Griffith first proposed the dilution of a few magnetic bonds in the PM matrix above the transition temperature in the range $T_{rand} < T < T_G$ (the reason for FM clusters) leads to the singularities in the free energy in certain Ising ferromagnets [73]. The pure system should have one transition temperature in the absence of any disorder. Whereas, transition temperature influenced the region of the system caused by the nonappearance of magnetic bonds in the disorder systems. Bray and Moore developed the new finding on several systems where the magnetic transition temperature is suppressed by

disorder from the conventional value T_G to T_C due to the distribution in exchange bonds [74]. Fig. 1.8 depicted the pictorial representation of a few missing magnetic ions at a few lattice sites of the FM system [73]. In Fig 1.8, the region where the magnetic ion is occupied is highlighted. The nonappearance of the magnetic ions successively lowers the strength of the structure and gradually leads to develop the magnetically ordered phase where the temperature should be lower than T_C for the ideal system. Thus, the new phase emergence between T_G and T_C which has the FM clusters in the PM background is called the GP. Thus, the exchange bond strength is J having the distribution probability p for the nearest neighbor magnetic ions whereas the non-magnetic with bond strength 0 has the probability (1-p) due to induced disorder. In the present case, below a critical percolation threshold pc, the co-operative ferromagnetism will not be established and created, since the theoretical probability for the formation of infinite percolating "backbone" is zero (or divergence of correlation length is not possible). Whereas for the scenario where p is larger than threshold pc, comparatively small ferromagnetism is generated because of the shortage of percolation path but essentially at a temperature T_G below the long-range FM ordering temperature of undiluted system T_G (@ p=1). There is also a presence of singularities in the thermodynamic quantity such as magnetization in the DPs phase region and thus it will not follow as an analytical function of fields. Hence, the system does not behave similarly to pure PM and also does acquire the LRO by generating an infinite percolating chain. Thereafter, a simplified discussion for different bond-distribution formed between 0 and J is introduced by Bray and Moore that finally suppresses the long-range magnetic ordering temperature T_G to Tc, which becomes very important to understand the GP in several magnetic systems [74]. Initially, Salamon et al reported the experimental realization of GP through the dc susceptibility measurement on a hole-doped manganite system [75]. GP is observed in many systems and it appears because of several reasons such as phase

separation, competition between FM and AFM interactions, presence of various sizes of clusters, and geometrically frustrated magnetic interactions. The disorder is one of the main reasons to show GP in the DP systems since they are the fundamental disordered systems because of having the different ionic radius and valence state at the B-site. Moreover, the presence of J-T distortion cations such as Mn^{3+} generates local distortion creating more disorder in the system. The dc susceptibility does not follow the CW law in the GP region, instead of it shows a sharp downturn behavior in inverse dc susceptibility above T_C considered a Hallmark of GP [75]. Indeed, the presence of a downturn or the sharp increase in susceptibility is the representation of the nucleation of FM clusters. The reason for the downturn behavior in the GP regime is that net moment inducing from the FM clusters suppresses the moment arising from the PM background at low field.

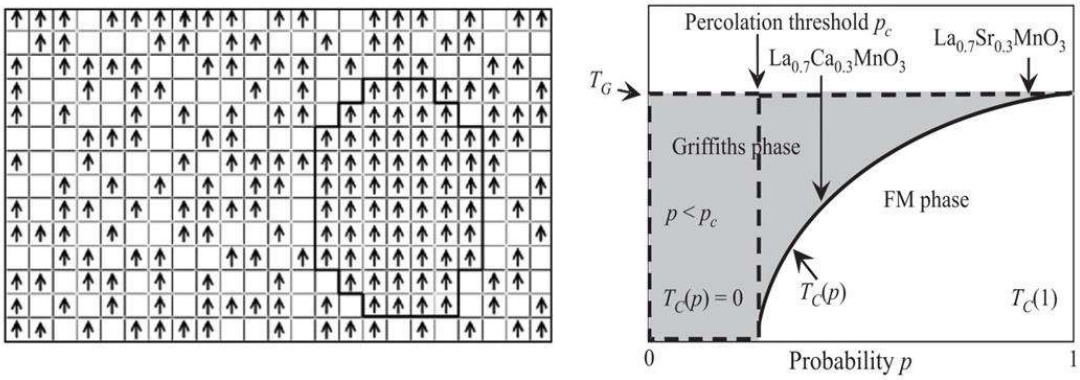

Fig. 1.8: (a) Pictorial view of a diluted ferromagnet where at some lattice sites the magnetic ions are missing and the outlined region shows the region in which all the magnetic ion sites are occupied. (b) A qualitative T-P diagram for a diluted FM material; here p is the possibility for the presence of an FM bond, the solid curve is a probable nature of the curie temperature $T_C(p)$ of a dilute ferromagnet. A conjectured position of $La_{0.7}Sr_{0.3}MnO_3$ with $T_C(p)$ ~370 K and $La_{0.7}Ca_{0.3}MnO_3$ with $T_C(p)$ ~220 K on the T-p diagram is shown.

On the other hand, the downturn behavior suppresses as the applied field is increased since the moment generated from the clusters is masked by the linear behavior arising from the

PM background moment at the high field. Thus, the GP temperature is the highest temperature where the downturn behavior is raised. And in that region inverse susceptibility behaves according to the following power law where λ is the non-universal exponent showing Griffiths singularity:

$$\chi^{-1} = (T-T_C^R)^{1-\lambda} \quad (1.20)$$

Here, the λ value lies between 0 and 1 which demonstrates the deviation from the standard CW law. In the PM region, λ will be zero generally and the above equation become normal CW law. Moreover, the correct estimation of the λ value greatly depends upon the choice of T_C^R. In general, the value of λ is obtained by the curve of $log_{10}(\chi^{-1})$ vs. $log_{10}(\frac{T}{T_C^R}-1)$. The λ value for GP ($\lambda_{GP}$) is estimated by the slope of the linear region of the curve just above T_C and λ_{PM} is estimated by the linear region of the slope above T_G.

1.4.4 Exchange Bias Phenomena:

EB can be shown by certain systems which have FM/AFM interfaces and cooled down to the Neel temperature (T_N) of the AFM where $T_C > T_N$. Due to this, an exchange anisotropy is introduced in the system that results in the EB effect. Experimentally, EB can be seen when the magnetization vs. field (MH) curve is shifted along the magnetic field as illustrated in Fig. 1.9.

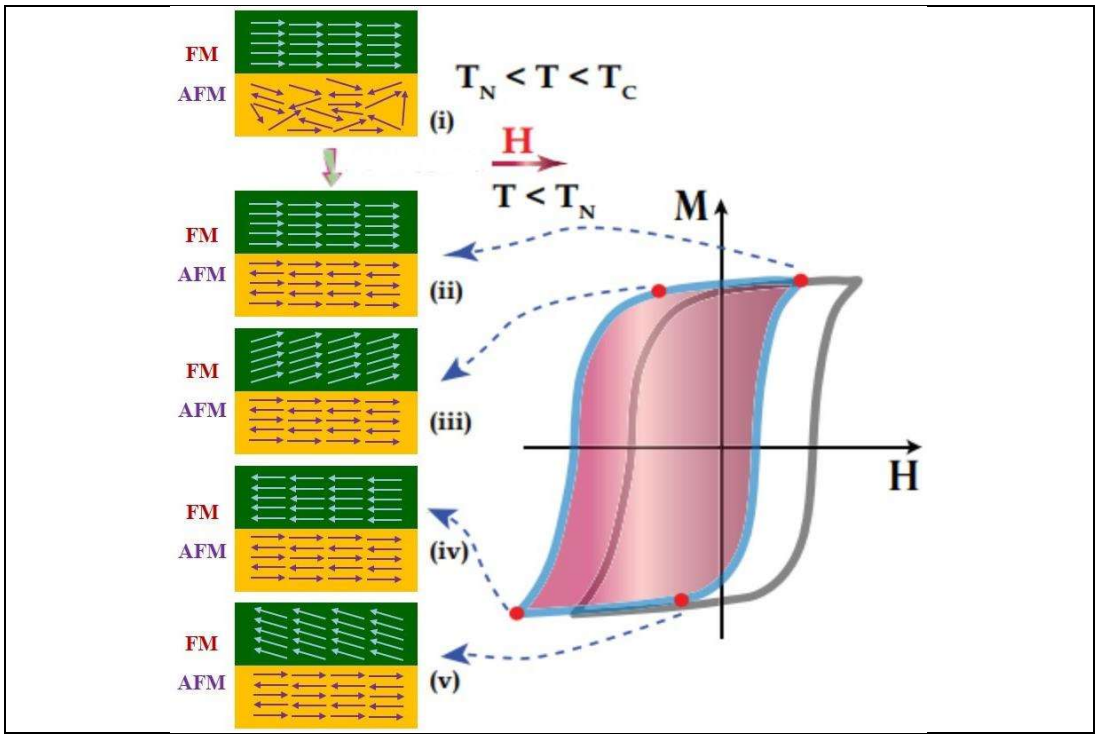

Fig. 1.9: Schematic representation of exchange bias effect.

The experimental realization of the EB effect by anisotropy is discussed by Meiklejohn and Bean in 1956 during the study of Co particles placed in their parent AFM oxide [76]. Later on, various systems having different FM and AFM layers exhibited the EB effect such as inhomogeneous materials, FM films coupled with AFM film, or with single crystal and small particles [77]–[79]. Thus, the EB phenomena can also be observed in several systems containing multiple magnetic phases for example hard/soft phase of FM, FM, and SG, FM and FIM, etc [79]–[82]. The unidirectional anisotropy and EB effect are manifested by observing an exchange interaction at the interface between the AFM and FM layers. The FM systems have spontaneous magnetization even in the absence of a magnetic field whereas the nearest neighbour exchange interaction is negative in the AFM materials. The description of the magnetic properties is visualized by the hysteresis loop and susceptibility data. Hence, the EB field (H_E) and coercivity (H_c) is estimated by $H_E=|H_{C1}+H_{C2}|/2$ and

$H_c=|H_{C1}+H_{C2}|/2$, here H_{C1} and H_{C2} represent the left and right coercive field values of the M(H) curve. We tried to explain the EB phenomena for better understanding as shown in Fig. 1.9 Firstly, under the application of the magnetic field, when the temperature is lowered than the T_C but higher than T_N ($T_N < T < T_C$) then the EB effect commences in the material because of the coupling of the interface at FM and AFM layers. Under the application of a magnetic field, AFM spins are randomly distributed in their PM state while FM spins are oriented along the direction of the applied field (stage i, (Fig. 1.9)). When the sample is cooled down below T_N, under the application of applied magnetic field, then the AFM monolayer of spins at interface coupled with FM spins starts oriented according to the FM spins along the direction of the magnetic field due to the exchange interaction. Whereas, the remaining spins in the AFM sublattice follow the AFM ordering and are aligned antiparallel to previous monolayers, thus producing zero net magnetization (stage ii, (Fig. 1.9)). The uncompensated spins at the interface of FM/AFM result in reasonable magnetization arising at the monolayer. Both FM and AFM will be in the one domain state when the magnetic field is reversed. During the opposite direction of the magnetic field, the FM spins rotate along the direction of the applied magnetic field while AFM spins are not able to rotate due to the large AFM anisotropy which prevents the alignment of AFM spins in the direction of applied. Thus, AFM spins remain unchanged at the FM/AFM interface (stage iii, (Fig. 1.9)). Although there is FM interaction at the boundary of FM/AFM, they attempted to orient FM spins to the previous direction. Additionally, a microscopic torque is generated at the interface by the AFM spins on FM spins which remain in their orientation ferromagnetically (stage iv, (Fig. 1.9)). Thus, an extra H is required to reverse the FM layer completely by suppressing the previous microscopic torque, when the FM state is in touch with the AFM layer. However, when this H is rotated back in its original previous direction, the FM spins will initiate to rotate at a smaller H

value, the reason being, that the microscopic torque by the AFM spins now aligns in the same direction as H (stage v, (Fig. 1.9)). As a consequence, the hysteresis loop shifted along the field axis, and the phenomenon is known as EB. The typical EB phenomena discussed above occur via applying a static magnetic field (H_{cool}) while cooling the sample and this type of EB is known as the conventional EB (CEB) effect. The shift of the loop is in the opposite direction from the applied cooling field and can be treated as the test of the EB effect. Intriguingly, EB can also be occurred in the absence of any applied magnetic field and is known as the spontaneous EB (SEB) effect. Recently, the observation of SEB seeks immense attention from researchers due to its feature and practical application as well. The systems having EB phenomena can be employed in various areas of practical application such as memory devices, storage devices, spintronics, etc [83].

1.4.5 Correlation between electronic structure and magnetism:

The magnetic nature of any system is depended upon the different exchange interactions present in that system. And for a better understanding of the different interactions (discussed in section 1.4.1) and complex states, prior knowledge of the electronic structure and spin state of elements present in the system is essential. It has a direct influence on the magnetic properties since different valence state has different magnetic moment and produce different exchange interactions. In particular, the electronic structure study for the oxides family having different transition metals has drawn great attention because of its ability to stabilize in different valence states as well as in different spin states i.e., different spin state degree of freedom [84]–[86]. For example, in general, Co/Mn/Fe/Ni transition metals can reside in 2+/3+/4+ oxidation states. Moreover, Co^{3+} ions, in an octahedral coordination, can exist in three possible spin states: a high spin (HS) state ($S = 2$, $t^4_{2g}e_g^2$), a low spin (LS) state ($S = 0$, $t^6_{2g}e^0_g$), and even an intermediate spin (IS) state ($S = 1$, $t^5_{2g}e^1_g$) which have the d^6 configuration, similarly for the Co^{2+} ions which have d^7 configuration

in octahedral coordination can possibly stay in HS state (S = 3/2, $t^5_{2g}e_g^2$) and in LS state (S = 1/2,$t^6_{2g}e^1_g$)[87]. Similarly, other transition metals also have various spin states such as Fe^{2+}, Ni^{2+}, $Cr^{2+,}$ etc. Moreover, particularly related to our work, the ordered DPs are FM insulators showing high-temperature magnetic ordering transition via the 180^0 FM super-exchange interactions between B^{2+} and B^{4+} ions (half-filled d orbital) and can be easily demonstrated by the Goodenough-Kanamori rule [15], [16]. For DPs, ASDs i.e., an interchange of B/B' sites are famously known to have well-known consequences on their physical properties, particularly on their magnetic properties which call for rigorous experimental and theoretical explorations of their electronic structure [8], [15], [88]. The ASD leads to significant deviations from ferromagnetism by producing additional AFM clustered regions. Moreover, the mixed valence state of transition metal also supports the ASD and creates AFM exchange interactions. All these AFM can be understood via superexchange interactions in the form of B^{2+}-O^{2-}-$B^{2+,}$ B^{3+}-O^{2-}-B^{2+}, B'^{4+}-O^{2-}-B'^{4+}, B^{3+}—O^{2-}—B^{3+}, B^{3+}—O^{2-}—B'^{3+} and B'^{3+}—O^{2-}—B'^{3} which further leads to the generation of competition between FM and AFM interactions [9]. In addition, the compounds having rare earth (4*f*) elements with magnetic properties, exhibit a broad range of intriguing properties because of the competing 4*f*-3*d* negative exchange interactions additionally due to the localized and complex configuration of the 4*f* orbitals as compared to the transition metal (3*d*) orbitals [89]–[91]. Thus, the study of the exact valence state is important to understand diverse interesting magnetic properties of the system and the magnetic anisotropy which leads to the competing complex interactions 3*d*-3*d*, 4*f*-4*f* consisting of isotropic, anisotropic symmetric, and anti-symmetric and 4*f*-3*d* super-exchange interactions. The prior knowledge of the electronic structure also helps us to give a good estimation of the total magnetic moment of the system. For this purpose, X-ray photoemission spectroscopy (XPS) spectra and X-ray absorption (XAS) spectra are the unique tools to probe into the

oxidation state of the constitutive elements present in the system. Moreover, XAS can also probe into the spin states of the system.

In addition, the nature of materials (semiconducting, metallic, and insulating) fundamental effect on the magnetic behavior and related mechanism. The electronic structure and the related physical properties can be yielded by the computational methods based on the density functional theory (DFT) and experimental analyses of the valence band (VB) spectra of XPS for the various materials. In different molecules and solids, we can observe various behaviour of physical phenomena such as orbital hybridization, band gap between the highest occupied molecular orbital and the lowest unoccupied molecular orbital, vertical ionization potentials, and electron affinities, that are essential for examining the correlated study between the electronic structures and physical properties [92], [93]. The multiple properties have been calculated based on the electron states in the electronic structure such as transition temperature, magnetic moment, Curie temperature, superconductor temperature, cohesive energy and melting point, etc. [94], [95].

1.4.6 Correlation between Raman study and magnetism (Spin-Phonon Coupling):

Raman spectroscopy is used as an important conventional and multifunctional probe to understand the local structural change, lattice dynamics, and spin-phonon coupling (SPC) in condensed matter physics. It is employed to investigate the qualitative and quantitative study of systems in various forms, such as bulk, thin film, nanostructure, or device. Moreover, Raman spectroscopy comparatively fast technique along with a wide range of characterization capabilities which also has a non-destructive nature and is extensively used in both fundamental science and application-oriented research.

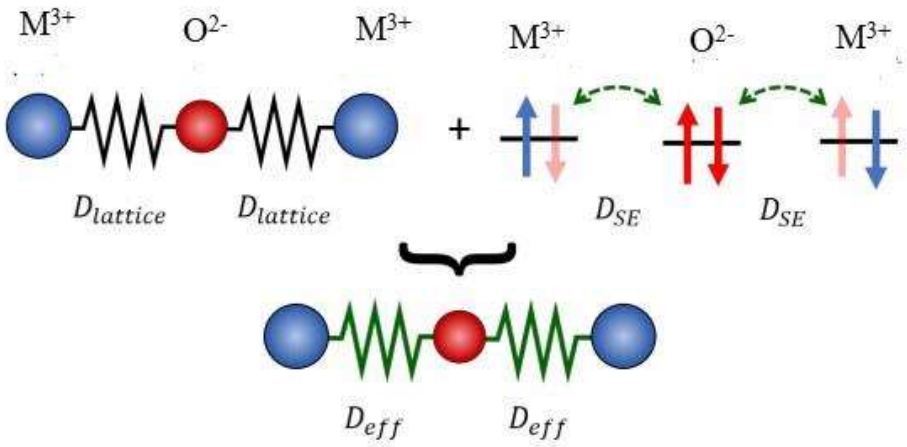

Fig. 1.10 A simple model for spin-phonon coupling: the Raman-active mode coupled by the spring constant $D_{lattice}$ modulates the M-O-M bond lengths.

SPC is realized in any system for each phonon by the renormalization of phonon frequencies with the intrinsic temperature dependence of the frequency and is treated as a key feature of SPC. Due to the involvement of the magnetic elements (M) in the lattice vibration, such as in the vibrations of oxygen ions in the M-O-M bonds, spin degrees of freedom are also taken into account to result in the modulation of the superexchange integral by the vibration. In addition to this, a few other mechanisms also play a significant role to modulate the phonon frequency such as charge order developed by magnetostriction can also be entangled in both degrees of freedom (spin and lattice) with each other. This can be simply understood by the model illustrated in Fig. 1.10 in which we have taken the example of transition metal (M) such as M^{3+}-O^{2-}-Mn^{3+} bond lengths. In the experimental temperature-dependent Raman spectra, the renormalization of the phonon frequency may be influenced by all these additional effects which can be seen as a deviation of the estimated behavior of the frequency from the Klemens model when the magnetic order occurs [96]. Hence, for the systems with magnetic atoms, thermal-variation of ω typically follows:

$$\omega(T) = \omega_0 + \Delta\omega_{latt}(T) + \Delta\omega_{anh}(T) + \Delta\omega_{e-ph}(T) + \Delta\omega_{s-ph}(T), \quad (1.21)$$

where, ω_0 represents the frequency at an initial temperature T_0, $\Delta\omega_{latt}$ is contribution arises because of the change in the ionic binding energies, due to the change of phonon frequency caused by the lattice expansion or contraction, $\Delta\omega_{anh}$ corresponds to the anharmonic contribution, $\Delta\omega_{e\text{-}ph}$ denotes the contributions from the electron-phonon coupling and $(\Delta\omega)_{s\text{-}ph}$ is the SPC, related to change in the exchange integral at magnetic sites by lattice vibration [97]. Moreover, if there is no structural change (local or global), SPC or electron-phonon coupling, or magnetostriction effect, ω usually follows the anharmonic equation, which is given as [98], [99]:

$$\omega_{anh}(T) = \omega_0 - C\left(1 + \frac{2}{e^{\frac{\hbar\omega_0}{2k_BT}} - 1}\right); \quad (1.22)$$

where C represents an adjustable fitting parameter, $\hbar$ denotes the reduced Planck's constant, and k_B is the Boltzmann's constant. By the anharmonic equation, the $\omega(T)$ curves should exhibit a hardening (increase in ω) with decreasing T, thereafter attaining a lower temperature plateau. Thus, the deviation from this behaviour at low temperature in the absence of any other effect is known as the SPC.

To understand the effect of magnetic ordering on phonon frequency, let us consider the example of a simple perovskite structure ABO_3, in which the B site transition metal is associated with an intermediate oxygen ion. The approach is also similar to other systems, where two different magnetic atoms are connected through oxygen. if the ions are displaced from their equilibrium positions, then the chemical bond abstracted as a mechanical spring with spring constant D, which mediates the restoring forces as described in the Fig. 1.10. If we take the region of the PM state then the magnetic moments are not oriented and non-correlated. In that case, the lattice potential $D = D_{lattice}$ is the only reason for the restoring

force. In the magnetic phase region, where the magnetic moments are correlated, the magnetic superexchanges interaction needs to be considered at lower temperatures. Since the superexchange interaction is directly linked with interionic distance therefore when the oxygen ion is perturbed from its equilibrium position, then the superexchange interaction is also changed. Then the effective spring constant has the contribution from both lattice potential and the superexchange potential $D = D_{lattice} + D_{SE}$ according to the mechanical model. Thus, the effective phonon frequency $\omega = \sqrt{}D/m$ is also influenced by this additional contribution, in the classical mechanical model. For a more quantitative approach, the quantum-mechanical models are also present in the literature which are able to investigate the SPC due to superexchange. For this Granado et. al., proposed the model that was described SPC in the A-type AFM $LaMnO_3$ based on the work of Baltensperger and Helman for EuO [97], [100]. They explained the detailed model of the Hamiltonian which suggests the magnetic interaction, and an expression of the exchange integral which is modulated by the ion displacements of the phonon modes, and then, their connection with the phonon frequency. Thus, the temperature-dependent Raman spectra provide an opportunity to shed light on the phonon renormalized and its correlation with magnetic ordering.

1.5 Motivation of the thesis:

Spin frustrated systems arising from the disorder are the fascinating and rising field of interest in condensed matter physics. The unconventional magnetic properties along with the correlated study of the charge and other degrees of freedom make them a suitable member for technological application. DPs are known as the disorder-driven spin frustrating system. The ordered DPs are FM in nature in contrast with their end members which are generally AFM (i.e. ABO_3 and $AB'O_3$) [9], [16]. While the spin frustration in the

system reaches a frozen SG state with random distribution after attaining a particularly critical level due to the ASD [9], [101]–[105].

The underlying mechanics behind such non-ergodic states are still less explored and complete knowledge of such randomly oriented magnetic states is an open challenge. In contrast, the presence of the quenched disorder sometimes leads to a glassy state at lower temperatures known as the RSG even after showing an LRO at higher temperatures. [18], [63], [106]. The studies exploring the RSG state are till limited to some extent as compared to the systems showing the SG states. Despite the extensive research interest in such systems to understand the nature and origin of such re-entrant glassy states, it stays contrivable.

Moreover, the quenched disorder is also famous to produce peculiar GP [10], [18], [73]–[75], [107]–[111]. Although the experimental realization of such a special phase after its theoretical anticipation was thought to be remote, the magnetic susceptibility study at different lower fields has provided a fine gauge for probing this GP [75]. In addition, the competition between FM/AFM interactions is also the manifestation of the EB effect as mentioned earlier. Thus, the systems having more than one phase are the potential candidate for arising the interesting phase known as the EB effect which can be seen by the horizontal or vertical shift in the M(H) loop. The EB effect is the result of the different exchange interactions at the interface between FM and AFM components [76], [112]–[114].

Furthermore, the phonon spectra of various DPs have been intensively studied and the role of A site rare earth element affects the SPC. Earlier Kumar et al. showed the role of the different ionic radius of A site rare earth effects the SPC such as get weakened from replacing the A site from La to Nd. Similarly, S. Kumar also proposed the significant effect of A-site on SPC by theoretical analyses on Y_2NiMnO_6 in the DPs system [115]. Since the

smaller ionic radius at the A site generates larger octahedral distortion that has an extensive effect on the coupling between the magnetic ordering and phononic degree of freedom.

In literature, the La and Y-based ordered DPs are widely explored relative to the Tb_2CoMnO_6 (TCMO) DP, therefore investigating its physical behavior may disclose some new intriguing phenomena [116], [117]. Moreover, for the last couple of decades, $TbMnO_3$ is intricately studied because of its magnetism-driven ferroelectricity which is one end member of TCMO DP [118]–[120]. Theoretical and experimental investigations have drawn much attention to this system for unraveling the origin along with the realization of the coupled behavior at elevated temperatures for the last two decades. Wheres, the other end member of TCMO, $TbCoO_3$ belongs to the $RCoO_3$ cobaltite family which is also extensively explored because of its thermally assisted spin-state transition of the Co^{3+} ions. Thus, in the present thesis, we have investigated the physical properties of the TCMO system such as electronic structure, Raman study, magnetic study, and as well as the correlation of each property.

For the next work, we have chosen the two different DP system such that one belongs to the disorder family with AFM ground state and the other belongs to the ordered family and exhibit FM ground state so that it will be a platform to occur EB phenomena with AFM background. The Pr_2CoMnO_6 (PCMO) has shown some fascinating magnetic and electronic properties of the ordered DP family while Pr_2CoFeO_6 (PCFO) belongs to the disorder DP family which exhibits exotic magnetic and electronic properties such as SPC, EB, GP, SG, and G-type magnetic ground state[18], [121]–[125]. The lattice disorder results in the formation of such intriguing phenomena. Thus PCMO and PCFO both the member of the ordered and disordered DP family respectively are rich in magnetic behaviour well as in structure and electronics properties[122], [125]. Therefore, with such a background, it will be interesting to investigate the magnetic properties, detailed Raman

spectroscopy along with the electronic structure by XPS and ab initio calculations (DFT) of $Pr_2CoFe_{0.5}Mn_{0.5}O_6$ (PCFMO).

As mentioned in section 1.3.2, the linear spin chain systems have been a very active field of interest from the experimental and theoretical aspects out of all the 1D spin systems. These spin chain systems have a strong correlation between the magnetic and the spin values [38], [126]. The integer spin chains possess gapped excitation and a robust ground state which provide them stability against magnetic order [44], [53], [127]. On the other hand, half-integer spin chains are gapless and even the slight interchain coupling leads to the long-range AFM order [128], [129]. Moreover, the occurrence of anisotropy results in a more complex nature and a richer phase diagram [130]. In this regard, Recently the $AM_2V_2O_8$ (A=Ba, Sr and M= Co, Mn, Ni, and Cu) class of materials are attracted a lot of attention and studied rigorously [51], [128], [131]–[133]. These materials have the screw chain along the c-axis forming by the MO_6 octahedral and distinct by the tetrahedral (VO_4) of non-magnetic ions [134]. Despite having the same structure as the entire $AM_2V_2O_8$ family, their magnetic nature depends upon the presence of different magnetic ions which leads to the different magnetic properties i.e., $BaCu_2V_2O_8$ (S =1/2) has a large spin gap of 230 K and is a 1D alternating spin chain system [51], [135] and when Cu is replaced by magnetic ion as $PbNi_2V_2O_8$ (S = 1) and $SrNi_2V_2O_8$ (S = 1) resides 1D Haldane spin-gap system [136], [137] while $SrMn_2V_2O_8$ (S = 5/2) is Heisenberg spin chain compound [138], $BaCo_2V_2O_8$ and $SrCo_2V_2O_8$ (S = 3/2) becomes 1D Ising spin systems and with large magnetic anisotropy [132], [139]–[141]. In addition, the $PbNi_2V_2O_8$ and $SrNi_2V_2O_8$ compounds confirmed the spin liquid behavior through various studies including different experimental methods such as magnetization, neutron scattering, nuclear magnetic resonance, and specific heat [128], [142], [143]. Thus, the compound might exhibit a quantum phase transition from the spin-liquid state to an ordered AFM state after applying

a small external or internal perturbation. Regardless of the appealing interactions between the lattice vibration and magnetism, the studies exploring the presence of SPC remain largely undiscovered in the linear spin chain system. To the best of our knowledge, out of all the members of the $AM_2V_2O_8$ family, only $SrMn_2V_2O_8$ and $BaMn_2V_2O_8$ (BMVO) have LRO transition is quite high (~42.2 K and 36 K) thus making them feasible to unravel the SPC in the system [138], [144]. However, the magnetic structure and easy axis of the BMVO compound are still unexplored whereas, for $SrMn_2V_2O_8$, AFM chains are along the *c* axis and are ordered ferromagnetically within the *ab* plane, as discussed by A. K. Bera et al. [131]. Thus, we choose BMVO to unfold its magnetic structure and plausible entanglement between spin and lattice vibrations in this brief report. To assess the interaction of spins and phonons, we investigated the temperature-dependent Raman scattering whereas for analyzing the magnetic ground state and magnetic order we performed detailed neutron scattering and magnetic measurements.